

Successive Phase Transitions of BaTiO₃ Ceramics Synthesized by Powder-calcination

Akihiro Hamano, Tooru Atake & Yasutoshi Saito*

Research Laboratory of Engineering Materials, Tokyo Institute of Technology,
4259 Nagatsuta-cho, Midori-ku, Yokohama 227, Japan

(Received 4 November 1987; accepted 4 December 1987)

ABSTRACT

The BaTiO₃ ceramics has been synthesized by calcining the powdered reactants BaCO₃ and TiO₂ at various temperatures, to examine the influences of calcination temperature on the successive phase transitions. The properties of the products have been studied by differential thermal analysis, dielectric measurements, X-ray diffraction and scanning electron microscopy. While the cubic–tetragonal transition temperature shifts towards higher temperatures with increasing calcination temperature, the lower two transitions shift towards lower temperatures. The thermal and dielectric anomalies due to the phase transitions increase as the calcination temperature rises.

1 INTRODUCTION

Barium titanium trioxide (BaTiO₃—perovskite type, so-called barium metatitanate or barium titanate) is one of the most important materials for ferroelectrics as it has a very high dielectric constant. In the synthesis of BaTiO₃ ceramics, the method of powder-calcination has been widely adopted. However, the properties of the products synthesized from powdered reactants are strongly influenced by the calcination conditions, because of the inhomogeneous mechanism in the solid state reaction. The aim of the present investigation is to clarify the interrelation between the properties of the products and the calcination process.

* To whom all correspondence should be addressed.

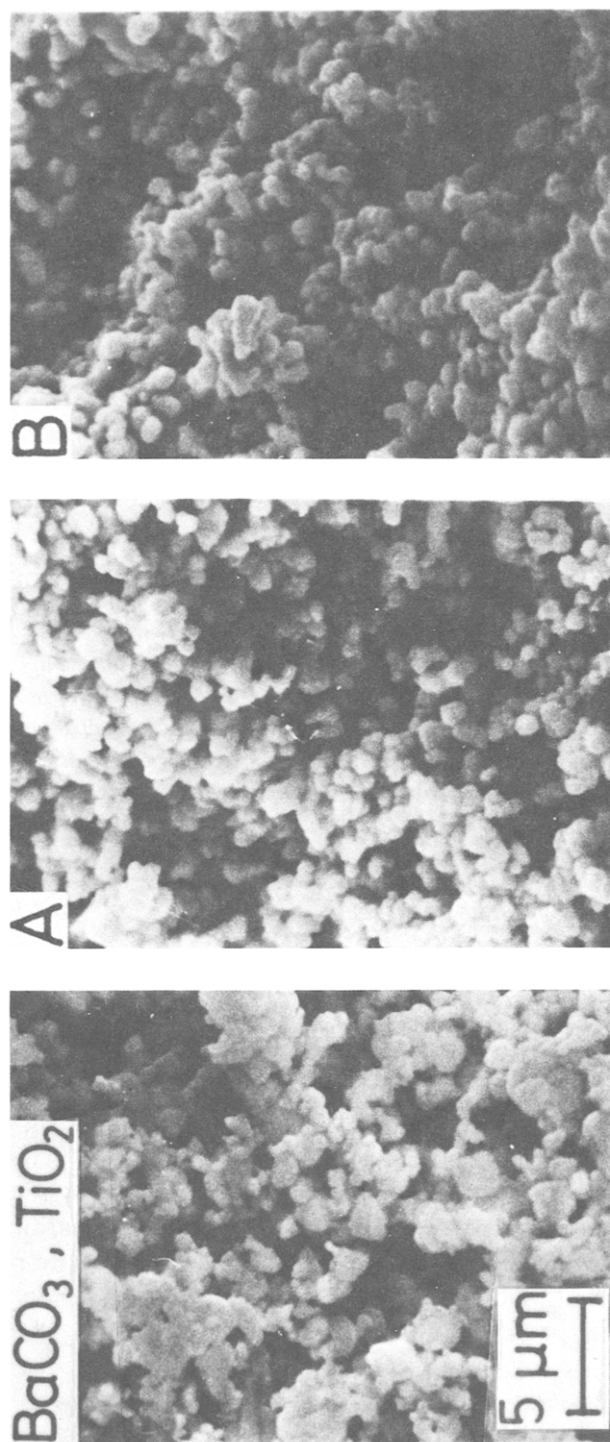


Fig. 1. Scanning electron micrographs of the starting mixture of BaCO_3 and TiO_2 , and the fractured surfaces of Samples A–D.

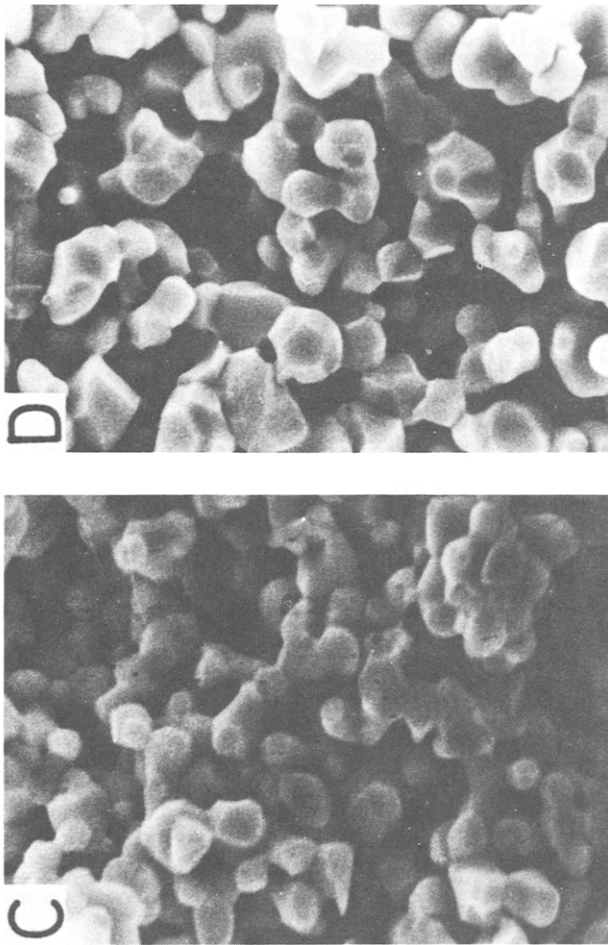


Fig. 1.—contd.

Barium titanate¹ is paraelectric above 397.72 K and the crystal structure is of a perovskite type (O_h^1 -Pm3m). On cooling from the paraelectric phase, the first-order phase transition of displacive type occurs and the crystal changes to the ferroelectric phase; the structure is tetragonal (C_{4v}^1 -P4mm). Below room temperature, two first-order phase transitions occur at 284.9 and 201.6 K;² the crystal structures are C_{2v}^{14} -Amm2 between the two phase transitions and C_{3v}^5 -R3m below 201.6 K, respectively. Such successive phase transitions in ferroelectrics have been studied extensively, and in particular BaTiO₃ is a typical example.

The present investigation has been made using differential thermal analysis, dielectric measurements, X-ray diffraction and scanning electron microscopy, focusing attention on the successive phase transitions in BaTiO₃.

2 EXPERIMENTAL

High purity starting materials, BaCO₃ (99.99%, Rare Metallic Co. Ltd, Tokyo, Japan) and TiO₂ (99.9%, rutile, High Purity Chemical Laboratory Co. Ltd, Saitama Prefecture, Japan), were weighed to a stoichiometric ratio and mixed in an alumina mortar by wet-grinding with ethanol. After air-drying at room temperature, the mixture was pressed into pellets (16 mm in diameter and *c.* 10 mm in thickness) at 80 MPa. The pellets were fired in an electric furnace for 43 ks at 1170 (Sample A), 1320 (Sample B), 1470 (Sample C) and 1620 K (Sample D). The apparent densities of the samples were 1.80 (A), 2.52 (B), 3.52 (C) and 3.92 (D) g cm⁻³; these values correspond to 30–65% of the theoretical density.

The fractured surfaces of the pellets were observed by using a scanning electron microscope. The powder X-ray diffraction patterns were obtained with a diffractometer using Ni-filtered CuK α radiation.

The differential thermal analysis (DTA) was performed between 90 and 470 K by using laboratory-made apparatus.³ The temperature difference between the sample and the reference material (α -Al₂O₃) was measured with thermocouple *E* (chromel versus constantan). A powdered sample of about 300 mg was loaded into a glass vessel, which was evacuated and sealed after introducing small amount of helium gas (30 kPa) for heat exchange. The cooling and heating rates were -0.04 – -0.06 K s⁻¹ and $+0.035$ – $+0.045$ K s⁻¹, respectively.

The method of dielectric measurement has been described previously.⁴ The measurements below room temperature down to liquid nitrogen temperature were carried out by using the laboratory-made cryostat.⁴ For the measurements above room temperature up to 570 K, a similar apparatus was newly constructed by using heat-resisting materials. The calcined pellets

were thinned to 1 mm by abrading the surfaces with SiC paper, and then cleaned in ethanol by using an ultrasonic washer. The dielectric constants were measured at 1 kHz under the electric field of 1 kV m⁻¹. The cooling and heating rates were about 0.02 K s⁻¹ which were small enough to neglect any thermal inhomogeneity in the sample.

3 RESULTS AND DISCUSSION

The scanning electron micrographs of the starting mixture and of the fractured surfaces of Samples A–D are shown in Fig. 1. It can be seen clearly that the grain size shows as the calcination temperature increases (Sample A–Sample D). The average sizes are estimated as 0.8, 1.0, 2.2 and 2.6 μm for Samples A–D, respectively.

The structural characterization was performed with powder X-ray diffraction. The results are reproduced in Fig. 2. All the diffraction patterns exhibit no extra peak attributable to any impurities. In the case of Sample A, the separation of the two lines of (002) and (200) is ambiguous. The patterns of this region are given in enlarged scale in Fig. 3. The (002) diffraction in Sample A is observed as a shoulder on the lower angle side of the (200) peak. Although it is hard to see precisely the location of the two peaks owing to the

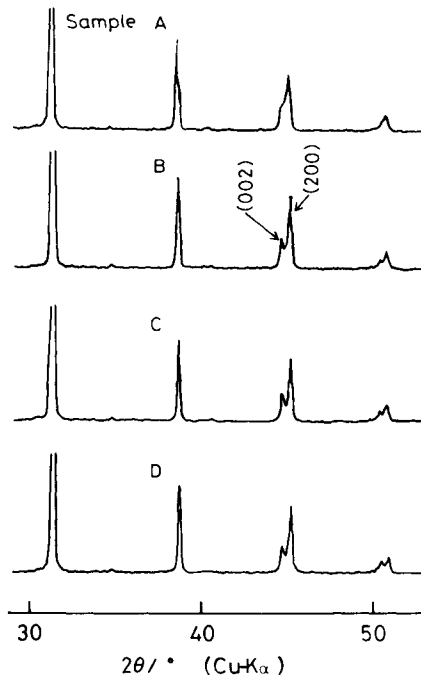


Fig. 2. Powder X-ray diffraction patterns of Samples A–D.

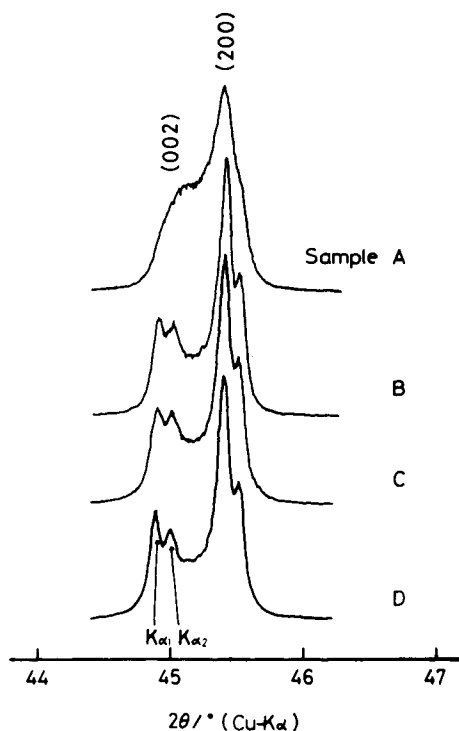


Fig. 3. Powder X-ray diffraction patterns of Samples A–D. Enlargement of the (002) and (200) lines.

broadening, the distance of the two peaks in Sample A is apparently closer than the distances in Samples B–D. In general, the broadening of the peak in powder X-ray diffraction is caused by the lattice strain and/or crystallite size effects.⁵ However, the shift of location is not explained by such a broadening mechanism, unless there exists some other kind of indirect effects. Arlt *et al.*⁶ have reported that the lattice gradually changes from tetragonal structure to pseudocubic structure for grain sizes $< 0.7 \mu\text{m}$. As the average grain size in Sample A is about $0.8 \mu\text{m}$, the shift of location of the two peaks (002) and (200) observed in the present experiment is reasonably related to the appearance of the pseudocubic lattice.

Figure 4 shows the temperature dependence of the dielectric constants without correction for porosity in the samples. Two anomalies are observed at about 200 and 285 K for Samples B–D in heating runs, while no anomaly is seen for Sample A. The dielectric anomaly due to the cubic–tetragonal transition at about 400 K is detected in all the samples as shown in Fig. 5. The transition temperatures obtained in the dielectric measurements are summarized in Table 1, where the temperatures are those corresponding to the maximum points of the dielectric anomalies. While cubic–tetragonal

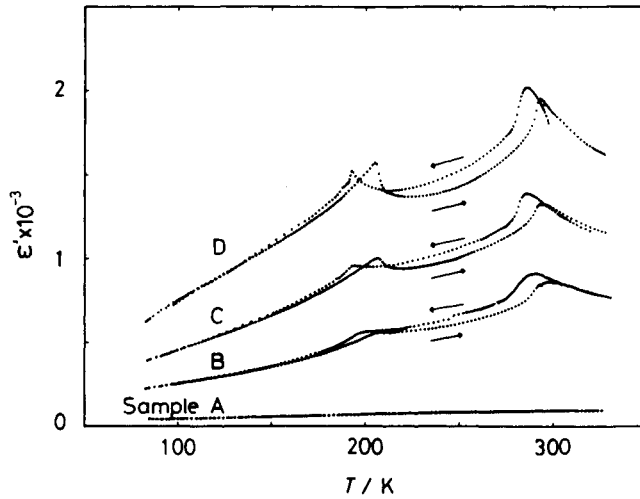


Fig. 4. Dielectric constants of Samples A–D, showing the anomalies at ~ 200 and ~ 285 K for Samples B–D.

transition shifts towards higher temperatures with increasing calcination temperature, the lower two transitions shift towards lower temperatures. These are probably due to the grain size effects.^{6–13} The shifts of transition temperatures have been reported by Kinoshita *et al.*¹⁰ with grain size changes between 1 and $50 \mu\text{m}$. Their data agree with the present results. It has been found^{7–9} that the grain size influences the internal stress in ferroelectric crystals. The stress due to deformation of cubic symmetry caused by passing through the ferroelectric transition is relieved by forming 90° twins in coarse-grained materials. In the case of fine-grained materials,

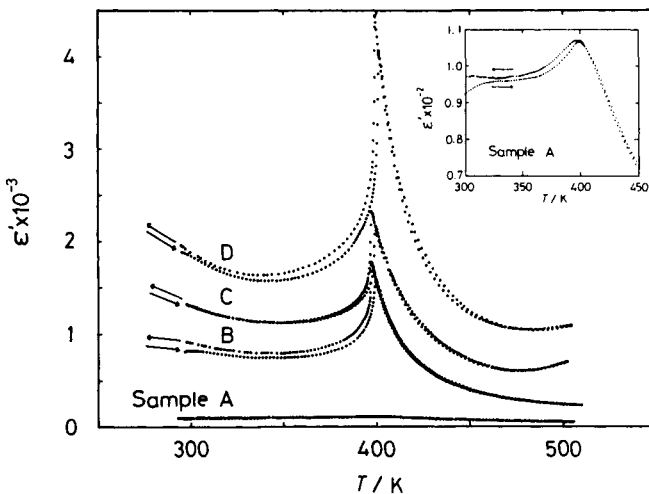


Fig. 5. Dielectric constants of Samples A–D, showing the anomalies at ~ 400 K.

TABLE 1
Transition Temperatures Determined by Dielectric Measurements in Heating and Cooling
Runs (the latter in parentheses)

	T_{tr} (K)		
	<i>Rhombohedral-orthorhombic</i>	<i>Orthorhombic-tetragonal</i>	<i>Tetragonal-cubic</i>
Sample A	—	—	399.1 (397.9)
Sample B	206.6 (197.6)	293.7 (288.5)	399.5 (397.2)
Sample C	206.4 (192.6)	293.7 (285.3)	399.7 (397.2)
Sample D	204.7 (192.2)	292.9 (285.5)	400.9 (398.9)

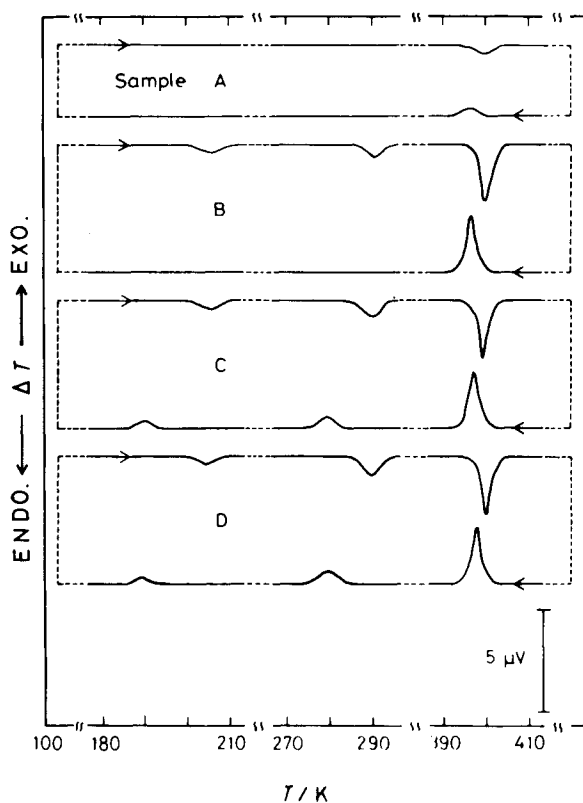


Fig. 6. DTA curves of Samples A-D.

however, there are very few 90° twins, and the stress remains. Such a stress may consist of uniform compression along the *c* axis and tension along the *a* and *b* axes. Bell *et al.*¹¹ explained such grain size effects in terms of an internal stress model. By considering the polarization dependent terms in the Devonshire free energy expression, they calculated the theoretical shift of transition temperature in various stress systems. The present results are also consistent with their findings.

The traces of the DTA experiments are presented in Fig. 6. For Sample A, only a small and broad anomaly is seen at about 400 K. In the case of Sample B, one anomaly is observed in the cooling run, while three anomalies are detected in the heating run. Three anomalies are clearly seen in both of the cooling and heating runs for Samples C and D. The area of the anomaly for Sample A at about 400 K is approximately 10% of the areas of the corresponding anomalies of Samples B–D, which compares favorably with the results of the dielectric measurements. The overall tendencies of the shifts in transition temperatures and of hysteresis phenomena are also in agreement with the results of the dielectric measurements.

REFERENCES

1. Hatta, I. & Ikushima, A., Temperature dependence of the heat capacity in BaTiO₃. *J. Phys. Soc. Japan*, **41** (1976) 558–64.
2. Todd, S. S. & Lorenson, R. E., Heat capacities at low temperatures and entropies at 298·16 K of metatitanates of barium and strontium. *J. Amer. Chem. Soc.*, **74** (1952) 2043–5.
3. Atake, T., Hamano, A. & Saito, Y., Characterization of powder-calcined BaZnGeO₄ by thermal analysis. *Thermochim. Acta*, **109** (1986) 267–74.
4. Kawaji, H., Saito, K., Atake, T. & Saito, Y., Phase transition at 211 K in crystalline barium nitrite hemihydrate. *J. Phys. Chem. Solids*, **47** (1986) 1085–8.
5. Hall, W., X-Ray line broadening in metals. *Proc. Phys. Soc.*, **A62** (1949) 741–3.
6. Arlt, G., Hennings, D. & De With, G., Dielectric properties of fine-grained barium titanate. *J. Appl. Phys.*, **58** (1985) 1619–25.
7. Buessem, W. R., Cross, L. E. & Goswami, A. K., Phenomenological theory of high permittivity in fine-grained barium titanate. *J. Am. Ceram. Soc.*, **49** (1966) 33–6.
8. Buessem, W. R., Cross, L. E. & Goswami, A. K., Effect of two-dimensional pressure on the permittivity of fine- and coarse-grained barium titanate. *J. Am. Ceram. Soc.*, **49** (1966) 36–9.
9. Pohanka, R. C., Rice, R. W. & Walker, Jr, B. E., Effect of internal stress on the strength of BaTiO₃. *J. Am. Ceram. Soc.*, **59** (1976) 71–4.
10. Kinoshita, K. & Yamaji, A., Grain-size effects on dielectric properties in barium titanate ceramics. *J. Appl. Phys.*, **47** (1976) 371–3.
11. Bell, A., Moulson, A. & Cross, L., The effect of grain size on the permittivity of BaTiO₃. *Ferroelec.*, **54** (1984) 147–50.

12. Hennings, D., Schnell, A. & Simon, G., Diffuse ferroelectric phase transitions in $\text{Ba}(\text{Ti}_{1-y}\text{Zr}_y)\text{O}_3$ ceramics. *J. Am. Ceram. Soc.*, **65** (1982) 539–44.
13. Kanata, T., Yoshikawa, T. & Kubota, K., Grain-size effects on dielectric phase transition of BaTiO_3 ceramics. *Solid State Commun.*, **62** (1987) 765–7.